Angewandte Chemie International Edition

Article

Liquid droplet formation and facile cytosolic translocation of IgG in the presence of attenuated cationic amphiphilic lytic peptides

Takahiro Iwata, Hisaaki Hirose, Kentarou Sakamoto, Yusuke Hirai, Jan Vincent V. Arafiles, Misao Akishiba, Miki Imanishi, Shiroh Futaki*

T. Iwata, Dr. H. Hirose, Dr. K. Sakamoto, Y. Hirai, Dr. J. V. V. Arafiles, Dr. M. Akishiba, Dr. M. Imanishi, Prof. Dr. S. Futaki
Institute for Chemical Research
Kyoto University
Uji, Kyoto 611-0011 (Japan)
E-mail: futaki@scl.kyoto-u.ac.jp

Abstract

Fc region binding peptide conjugated with attenuated cationic amphiphilic lytic peptide L17E trimer [FcB(L17E)$_3$] was designed for immunoglobulin G (IgG) delivery into cells. Particle-like liquid droplets were generated by mixing Alexa Fluor 488 labeled IgG (Alexa488-IgG) with FcB(L17E)$_3$. Droplet contact with the cellular membrane led to spontaneous influx and distribution of Alexa488-IgG throughout cells in serum containing medium. Involvement of cellular machinery accompanied by actin polymerization and membrane ruffling was suggested for the translocation. Alexa488-IgG negative charges were crucial in liquid droplet formation with positively charged FcB(L17E)$_3$. Binding of IgG to FcB(L17E)$_3$ may not be necessary. Successful intracellular delivery of Alexa Fluor 594-labeled anti-nuclear pore complex antibody and anti-mCherry-nanobody tagged with supernegatively charged green fluorescence protein allowed binding to cellular targets in the presence of FcB(L17E)$_3$.

Key words

antibodies; intracellular delivery; liquid droplet; liquid-liquid phase separation (LLPS); peptides

Introduction

Intracellular delivery of biomacromolecules is a central focus in the life sciences.[1] New approaches to deliver chemically modified proteins into cells would provide new opportunities to analyze and modulate cell functions. This would undoubtedly have great impacts on chemical biology, bioimaging, and related research. The delivery of therapeutic proteins is also important, considering the promise of antibodies, including immunoglobulin G (IgG) and their engineered segments, such as single chain antibody (scFv), as molecular targeting drugs.[2] Although numerous approaches have been developed to facilitate the delivery of proteins into cells, there are still many opportunities for improved efficacy, especially in the delivery of large proteins like IgG (150-160 kDa).[3]

Our research group has been developing a series of attenuated cationic amphiphilic lytic (ACAL) peptides to deliver IgGs and other functional proteins into cells.[4] Negatively charged amino acids such as glutamic acid (Glu) are placed in the potential hydrophobic faces of these lytic peptides. Using the designed ACAL peptides, efficient cytosolic delivery of monoclonal antibodies was achieved, allowing binding their intracellular targets and modulation of signal transduction.[4a, 4d, 4e] This was accomplished simply by mixing IgG with the ACAL peptides. More sophisticated delivery systems may be established by using appropriate means of complex formation

or packaging, because IgG should be localized together with the ACAL peptides permeabilizing the membranes to attain cytosolic translocation.

In this study, we thus endeavored to formulate IgG with the ACAL peptide L17E. To increase the local concentration of L17E to facilitate the more efficient permeation of IgG through membranes, a trimer of L17E was employed. For easy formation of a complex with IgG, the trimer was tagged with an Fc binding peptide (Fig. 1A, FcB(L17E)$_3$). To assess cytosolic translocation, IgG was fluorescently labeled with Alexa Fluor 488 (IgG-Alexa488).

We found that mixing FcB(L17E)$_3$ with IgG-Alexa488 resulted in the formation of liquid droplets or coacervate, which allowed efficient cytosolic IgG translocation. The addition of negative charges on IgG by modification with Alexa Fluor 488 proved critically important in liquid droplet formation. This liquid droplet-mediated intracellular translocation of IgG was not attained by simple pore formation in the cell membrane (plasma membrane) by the peptide. The need for energy-dependent and actin-driven membrane dynamics induced by the liquid droplet was suggested from pharmacological inhibitor experiments. The potential applicability of this approach to other proteins modified with negatively charged molecules was exemplified by the successful delivery of anti-nuclear pore complex antibody (modified with Alexa Fluor 594) and anti-

mCherry-nanobody (tagged with supernegatively charged green fluorescence protein ((–

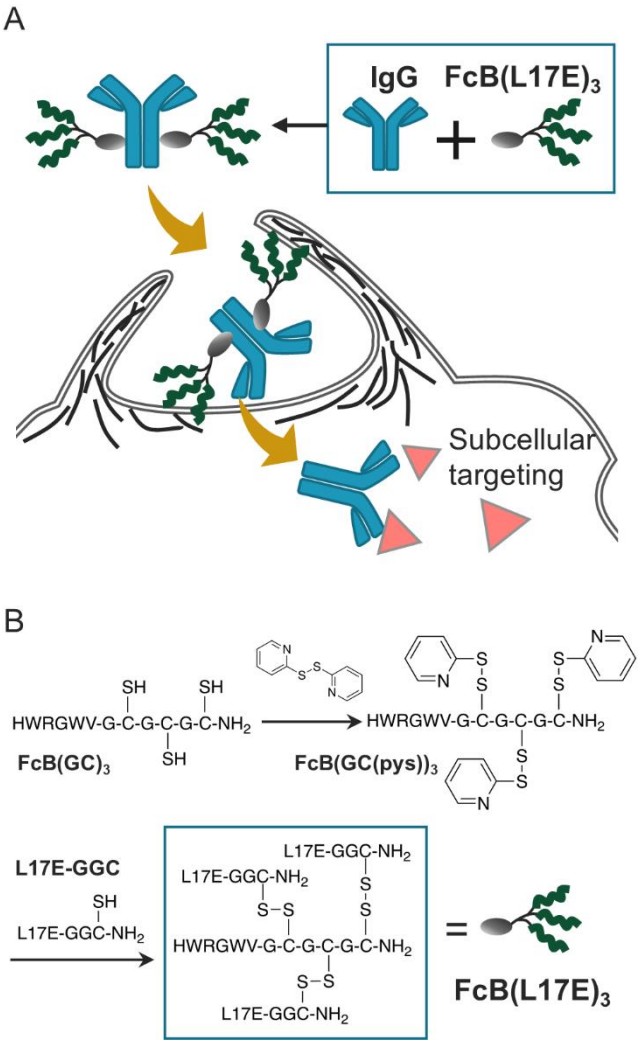

30)GFP) was demonstrated.

Figure 1. (A) Possible delivery system of IgGs into cells using the L17E trimer conjugated with an Fc binding peptide [FcB(L17E)$_3$]. L17E allows permeation of IgGs though the membrane. (B) Preparation of FcB(L17E)$_3$. Further details of FcB(L17E)$_3$ preparations are provided in the Supporting Information.

Results & Discussion

Design and preparation of the complex of IgG and L17E trimer

We previously reported the ability of L17E to deliver antibodies (IgGs) and other bioactive proteins into living cells.[4a] Simply applying mixtures of L17E and IgG to cells led to the recognition of intracellular target proteins and modulation of signal transduction. This highlighted the impact of this peptide on intracellular delivery. L17E was designed based on the sequence of the cationic amphiphilic spider-toxin peptide M-lycotoxin,[5] which has a high membrane-lytic activity. Replacing the Leu residues at position 17 of M-lycotoxin with a negatively charged Glu reduces the hydrophobicity and attenuates the lytic activity of L17E on cell membrane. However, the recovery of the membrane lytic activity in the following endocytic processes results in efficient cytosolic translocation of the molecules to be delivered into cells. Multiple L17E molecules may be necessary to enhance membrane permeabilization to allow the permeation of large proteins, such as antibodies (e.g., IgGs). Multimerization is a practical strategy to enhance the membrane interaction of peptides.[6] In fact, dimerization of L17E allows more efficient membrane permeation of large molecules compared with the L17E monomer.[4e] As described above, complex formation of the L17E multimer with IgGs is a practical approach to facilitate cytosolic translocation of IgGs. Therefore, we designed a trimer of L17E using a 6-residue

Fc region binding peptide (FcBP; HWRGWV)[7] as an attachment linker to IgG (Fig. 1A).

Binding of peptides to the Fc regions of IgG have been employed to yield IgG conjugates/complexes of defined numbers of attached molecules at specific sites of modification, as exemplified in the preparation of antibody-drug conjugates.[8] The use of shorter lengths of FcBPs may benefit the preparation of the conjugates with three molecules of L17E, which has 25 amino acid residues. Thus, the 6-residue FcBP was employed.

FcBP conjugated with three molecules of L17E [FcB(L17E)$_3$] was prepared by disulfide formation among these segments (Fig. 1B; detailed peptide structures are given in Table S1). FcBP bearing tri-glycylcysteinyl moieties on the C-terminal [FcB(GC)$_3$] was prepared and the cysteines in the sequence were activated by treatment with 2,2'-dithiodipyridine [FcB(GC(pys))$_3$, pys = 2-pyridinesulfenyl].[9] L17E bearing a glycylglycylcysteinyl moiety on the C-terminal (L17E-GGC) was also prepared and treated with FcB(GC(pys))$_3$. Purification of the product using reverse-phase high-performance liquid chromatography (RP-HPLC) yielded pure FcB(L17E)$_3$. The mass was confirmed by matrix-assisted laser desorption/ionization time-of-flight mass spectrometry (MALDI-TOFMS).

Particle-like structure formation and influx into cytosol of Alexa Fluor 488-labeled IgG mixed with FcB(L17E)$_3$

Next, we evaluated the efficacy of cytosolic IgG delivery in complex with FcB(L17E)$_3$. Prior to this, the cytotoxicity of FcB(L17E)$_3$ was analyzed using the WST-8 assay, which assesses mitochondrial metabolic activity.[10] HeLa cells were treated with varying concentrations of FcB(L17E)$_3$ (0.1 – 10 μM) for 1 h in α-minimum essential medium supplemented with 10% bovine serum [serum containing medium, hereafter denoted as α-MEM(+)]. No marked cell death was observed after treatment with ≤ 1 μM FcB(L17E)$_3$ (Fig. S1). Thus, 1 μM FcB(L17E)$_3$ was used for the following experiments.

The ability of FcB(L17E)$_3$ to deliver IgG to the cytosol was analyzed using Alexa Fluor 488-labeled IgG (Alexa488-IgG) by confocal laser scanning microscopy (CLSM). To prepare the complex of Alexa488-IgG with FcB(L17E)$_3$, Alexa488-IgG and FcB(L17E)$_3$ were incubated in phosphate-buffered saline (PBS) at a molar ratio of 1:2 (FcB(L17E)$_3$ = 14 μM) for 30 min. The mixture was diluted with α-MEM(+) to yield final FcB(L17E)$_3$ concentration of 1 μM (Alexa488-IgG = 0.5 μM; 75 μg/mL). HeLa cells were incubated with this mixture for 30 min at 37°C.

Diffuse cytosolic labeling by Alexa488-IgG was observed in over 60% of cells following treatment with a mixture of Alexa488-IgG and FcB(L17E)$_3$ (1:2), indicating

effective Alexa488-IgG cell delivery (Fig. 2A, +75 μg/mL Alexa488-IgG, FcB(L17E)$_3$). A mixture with 40 μM L17E instead of 1 μM FcB(L17E)$_3$ produced cytosolic Alexa488-IgG signals in only 5% of cells (Fig. 2A and B; +75 μg/mL Alexa488-IgG, L17E). Signals were detected in 40% of cells, even at an Alexa488-IgG concentration of 1 mg/mL (Fig. 2A and B; + 1 mg/mL Alexa488-IgG, L17E). Treatment with FcB(L17E)$_3$ resulted in signals in an increased percentage of cells and more intense cytosolic Alexa488-IgG signals. No cytosolic Alexa488-IgG signals were observed in cells treated with 75 μg/mL Alexa488-IgG alone (in the absence of delivery peptide) (Fig. 2A and B; no peptide). These results indicate a marked improvement in cytosolic IgG delivery efficacy with the use of FcB(L17E)$_3$.

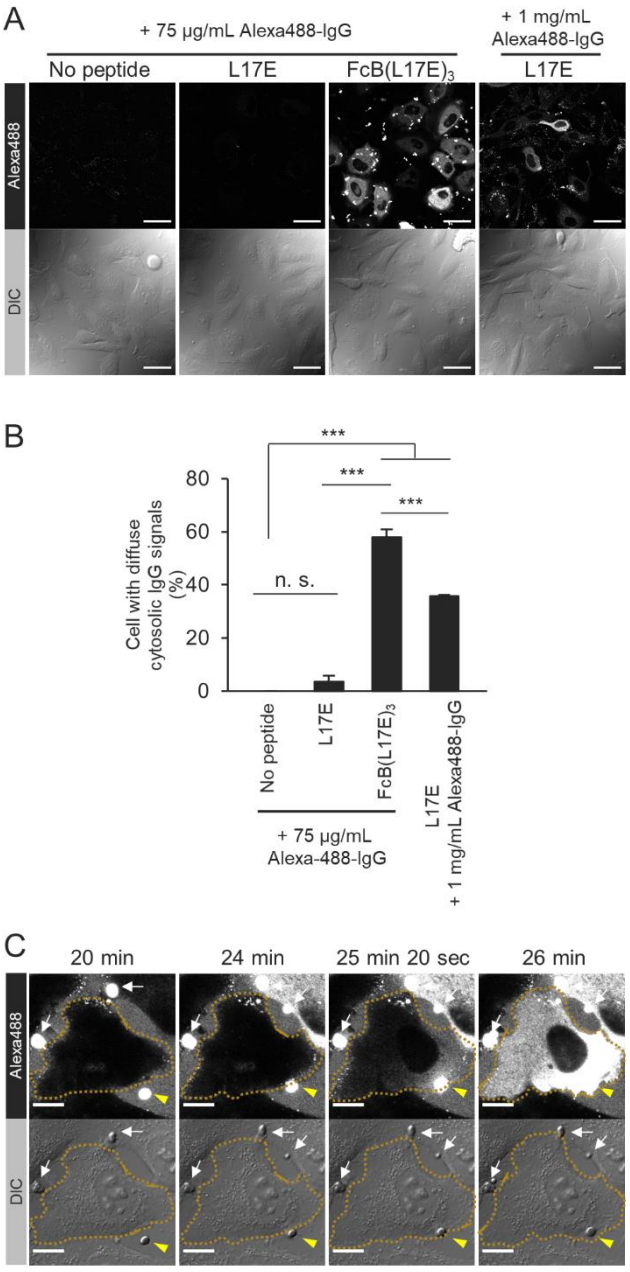

Figure 2. Cytosolic delivery of Alexa488-IgG by FcB(L17E)3. A) Cytosolic appearance of Alexa488-IgG after treatment with L17E (40 μM) or FcB(L17E)3 (1 μM) in α-MEM(+) for 30 min. Scale bar denotes 40 μm. B) Percentage of cells displaying diffuse cytosolic IgG signals. Results are presented as mean ± standard error (SE) (n=3). ***; $p<0.001$, n.s.; not significantly different by Tukey-Kramer's honestly significant difference test. C) Time-lapse imaging of cells treated with a mixture of Alexa488-IgG

with FcB(L17E)$_3$. The imaging interval was 20 sec. Scale bar denotes 10 μm. Arrows indicate the sedimentation of particle-like structures on culture dishes, which eventually contact with cell membrane and led to the distribution of Alexa488-IgG signals inside cells. The particle-like structure with yellow arrowhead represents a particle-like structure typically yielding influx of Alexa488-IgG into the cell (the cell boundary is highlighted with a dotted line).

Time-lapse imaging of cells treated with the mixture of Alexa488-IgG and FcB(L17E)$_3$ was performed to analyze the modes of FcB(L17E)$_3$ delivery of Alexa488-IgG into the cell interior in more detail. No notable cytosolic Alexa488-IgG signals were observed in the first 15 to 20 min. However, sedimentation of particle-like structures with a diameter of approximately 2 μm became evident on the culture dishes approximately 20 min after the addition of Alexa488-IgG/FcB(L17E)$_3$ mixture (Fig. 2C, 20 min, arrows and arrowheads). These structures were visible in both fluorescent and differential interference contrast (DIC) imaging. Some of these structures eventually contacted the cell membrane. Unexpectedly, attachment of these particles to cell membranes led to an immediate influx of fluorescent signals into cells and signal spread throughout the cells, as seen for the particle-like structure with arrowheads in Fig. 2C at 25 min 20 s and at 26 min and Supporting Information Video 1. These results suggest the possible encapsulation of Alexa488-IgG in the particles, allowing immediate influx of Alexa488-IgG into the cytosol upon the attachment of the particles to cells. This process requires energy-driven

cellular systems. No cytosolic Alexa488-IgG signals were observed after treatment at 4°C (Fig. S2), eliminating the possibility that the cytosolic influx of Alexa488-IgG was not due to simple pore/rupture formation in plasma membranes.

The importance of the potential lytic activity of L17E in delivery was confirmed using FcB(L9E)$_3$. L9E was also mutated from M-lycotoxin, having the same amino acid composition as L17E (in which the leucine at position 9 was substituted with glutamic acid instead of leucine 17 in L17E), but with very little cytosolic delivery activity.[4a] FcB(L9E)$_3$ was similarly prepared as in the case of FcB(L17E)$_3$ (Table S1). Although a mixture of FcB(L9E)$_3$ and Alexa488-IgG formed particle-like structures (Fig. S3A), no detectable level of cytosolic Alexa488-IgG was detected by CLSM analysis (Fig. S3B, C).

As a proposed mechanism of action, L17E attains transient permeabilization of cell membranes following the induction of actin polymerization and membrane ruffling.[4b] We hypothesized that a similar mechanism may be involved in the influx of Alexa488-IgG into cells. To assess this, HeLa cells expressing Lifeact-mCherry [11] were used. Lifeact is a 17-residue actin-binding peptide that is frequently used for live-cell imaging of cellular actin dynamics. Fused with mCherry, the organization of actin in live cells can be monitored in real time. HeLa cells expressing Lifeact-mCherry were treated

with a mixture of Alexa488-IgG and FcB(L17E)$_3$ (Fig. S4). Transient but intense Lifeact-mCherry signals immediately accumulated at the contact site where the particle-like structure was attached to the cell membrane (Fig. S4; mCherry, and DIC, 20 s; see also Supporting Information Video 2). This was followed by the influx of Alexa488 signals into cells from the area of particle attachment (Fig. S4; Alexa488, 40 s), leading to the spread of the signals into the cell interior (Fig. S4; Alexa488, 60 s). Importantly, these observations were complete within 1 min. These results imply that the interaction of the particle with the cell membrane leads to the induction of transient and local actin-structural alterations, accompanied by ruffling of the cell membrane.[12] This might lead to internalization of the particles or cellular membrane permeabilization by FcB(L17E)$_3$, followed by translocation of Alexa488-IgG into the cytosol.

Transient permeabilization of membranes following induction of actin polymerization and membrane ruffling is considered a major mode of action of L17E, which allows cytosolic delivery of IgG. It seems likely that cytosolic Alexa488-IgG influx in the presence of FcB(L17E)$_3$ may occur at least partially in the same manner as L17E-mediated cytosolic IgG delivery. The possible involvement of the cytoskeletal actin that was suggested by the results of Figure S4 was confirmed by cytochalasin D (CytoD) treatment. CytoD is a typical inhibitor of actin polymerization.[13] Cytosolic influx of

Alexa488-IgG was completely blocked in the presence of CytoD (Fig. S5 A and B). Similar to L17E-mediated cytosolic IgG delivery, there was also a significant decrease in the cytosolic Alexa488-IgG influx in the presence of FcB(L17E)$_3$ upon treatment with 5-(*N*-ethyl-*N*-isopropyl)amiloride (EIPA) (Fig. S5 C and D). EIPA inhibits Na^+/H^+-exchange, which in turn inhibits the induction of membrane ruffling.[14]Wortmannin is a phosphatidylinositol-3 kinase (PI3K) inhibitor that prevents the closure of membrane ruffles to form macropinosomes.[15] L17E-mediated cytosolic delivery was not inhibited by treatment with wortmannin,[4b] but FcB(L17E)$_3$-driven cytosolic Alexa488-IgG delivery was significantly inhibited (Fig. S5E and F). These observations may suggest that particle-like structures are internalized by macropinocyosis or the related mechanisms followed by cytosolic delivery of Alexa488-IgG, probably due to the membrane lytic activity of L17E moieties.

Coacervate formation of Alexa488-IgG in the presence of FcB(L17E)$_3$ and the importance to cytosolic distribution

In the preceding experiment, marked formation of particle-like structures occurred upon mixing of Alexa488-IgG with FcB(L17E)$_3$, leading to a marked influx of Alexa488-IgG into the cytosol. The results suggested the involvement of actin

polymerization and membrane ruffling, reminiscent of L17E-mediated IgG delivery into cells, indicating that the influx of Alexa488-IgG was not a simple membrane perturbation or pore formation by the treatment.

In the above experiments, Alexa488-IgG with FcB(L17E)$_3$ was mixed in PBS at a molar ratio of 1:2 (FcB(L17E)$_3$ = 14 μM) followed by dilution with α-MEM(+) to yield a final concentration of FcB(L17E)$_3$ (1 μM). The findings prompted the questions of whether each of the components was needed, and if mixing at a high concentration is needed for particle-like structure formation.

To answer the first question, 7 μM Alexa488-IgG and/or 14 μM FcB(L17E)$_3$ were incubated in 25 mM HEPES (pH 7.5) for 30 min, followed by dilution with a 4-fold volume of 25 mM HEPES (pH 7.5) to enable CLSM analysis. Although particle-like structures were formed in the presence of both Alexa488-IgG and FcB(L17E)$_3$ (Fig 3A), the lack of the counterpart (i.e., Alexa488-IgG alone and FcB(L17E)$_3$ alone) resulted in the lack of the particle-like structures (Fig S6). These results also suggest that serum is not required for particle formation.

To answer the second question, a mixture of Alexa488-IgG and FcB(L17E)$_3$ was prepared to immediately yield the final concentration by skipping the pre-mix step at high concentrations (Fig. S7B; Method 2). Fig. S7A (Method 1) represents the preparation

method of a mixture of Alexa488-IgG and FcB(L17E)$_3$ as used in Fig. 2 (i.e., mixed at an FcB(L17E)$_3$ concentration of 14 μM prior to dilution to 1 μM). Observation of the mixture prepared using Method 1 detected the formation of particle-like structures (Fig. S7C, left panel). No particle-like structures were formed in the mixture prepared using Method 2 (Fig. S7C, right panel). The efficacy of particle formation was in accordance with the efficacy in cytosolic Alexa488-IgG distribution. A mixture of Alexa488-IgG and FcB(L17E)$_3$ was prepared using Method 2 (Fig. S7B), which did not yield notable cytosolic Alexa488-IgG signals (Fig. S7D). Considering that FcB(L9E)$_3$ failed to deliver Alexa488-IgG into cytosol while it formed liquid droplets (Fig. S3), we concluded that both droplet formation and potential lytic activity possessed by L17E are important for the efficient cytosolic delivery of Alexa488-IgG.

In recent years, liquid-liquid phase separation (LLPS) has attracted considerable research interest as a means of formulating therapeutic proteins.[16] LLPS, also termed coacervation, occurs via numerous transient, noncovalent, and intermolecular interactions. The result is a two-phase separation consisting of a condensed droplet phase (i.e., coacervate) and an aqueous phase.[16b, 17] Protein encapsulation by LLPS is a spontaneous process that does not involve the use of organic solvents. This avoids denaturation of proteins in the formulation. Moreover, proteins condensed into coacervates preserve their

bioactivity as they are separated from their surroundings.[16a, 16b] Other characteristics of coacervation include inner fluidity, exchange of molecules with surroundings, growth by incorporation of polymer, and fusion with another coacervate that differs from aggregation.[18] Considering the potential of the above particle-like structures for facile protein delivery into cells, we evaluated if the particle-like structures shared the features of coacervates.

The fusion of droplets to form a larger droplet is the criterion for coacervates. This was confirmed by the sequential observation of droplets formed by FcB(L17E)$_3$ and Alexa488-IgG in 25 mM HEPES buffer (pH 7.5) (Fig. 3B). Furthermore, the driving force of LLPS is mainly electrostatic, π-π, and cation-π interactions between positively charged, negatively charged, or aromatic residues in the polymers.[17] The addition of NaCl or 1,6-hexanediol (1,6-HD) to coacervates should decrease the stabilization of droplets, leading to the collapse of LLPS.[19] A decrease in the size and number of droplets produced by FcB(L17E)$_3$ and Alexa488-IgG was observed by CLSM along with an increase in the concentration of NaCl and 1,6-HD, respectively (Fig. 3C, D; inset images). Turbidity is also a measure of coacervate formation.[20] Marked decreases in the absorbance at 650 nm of the solutions were evident with increases in NaCl and 1,6-HD concentrations (Fig. 3C, D). It should be noted that a certain fraction of droplets still exists at 150 mM NaCl

(*i.e.*, a comparable ionic strength in cell culture medium) (Fig. 3C), ensuring that the particle-like structures observed in Fig. 2 were liquid droplets.

We also evaluated the effect of 2,5-hexanediol (2,5-HD) on the stability of the liquid droplets, which is known to disrupt liquid droplets at a lesser extent to that of 1,6-HD (Fig. 3D, S8).[19c] In contrast that 1,6-HD had a notable effect on melting the liquid droplet structure (Fig. 3D), only marginal effect was observed for 2,5-HD (Fig. S8). Additionally, we performed fluorescence recovery after photobleaching (FRAP) on the droplets. FRAP is often employed to determine the molecular dynamics and mobility of fluorescent components in the phase-separated liquid droplets. Although fluorescence recovery is often attained in a few min or the less,[21] the recovery in the droplets formed by FcB(L17E)$_3$ and Alexa488-IgG was considerably slower. No marked recovery was obtained even after 10 h post-photobleaching (Fig. S9; see also Supporting Information Video 3). The results of 2,5-HD and FRAP experiment suggests adequate interaction between Alexa448-IgG and FcB(L17E)$_3$ to retain droplet structure in extracellular media, while allowing cytosolic Alexa488-IgG influx upon attachment to cell membrane. These features may add to the potentials of the liquid droplets as a mean of formulation for intracellular antibody delivery.

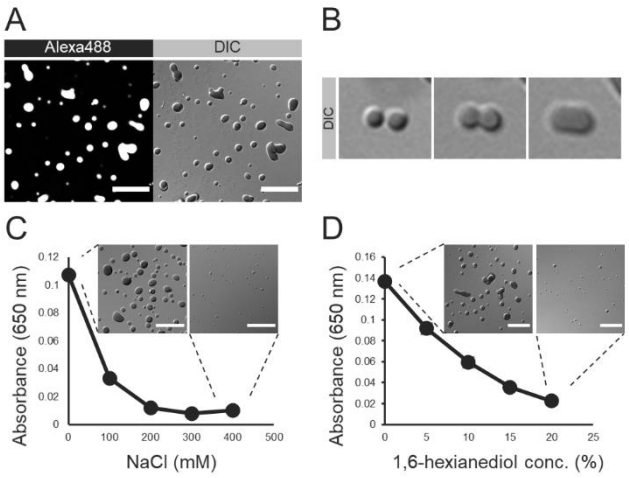

Figure 3. FcB(L17E)$_3$ forms coacervates with Alexa488-IgG. A) DIC imaging of the liquid droplets in a solution containing FcB(L17E)$_3$ and Alexa488-IgG. B) Time-lapse imaging of the fusion of liquid droplets made by FcB(L17E)$_3$ with Alexa488-IgG. The examination interval was 5 min. C) and D) The absorbance at 650 nm of the solution containing FcB(L17E)$_3$ and Alexa488-IgG in the absence and presence of NaCl or 1,6-hexanediol (1,6-HD). Results are presented as mean ± standard deviation (SD) (n=3). The inset shows CLSM imaging of the droplets in the absence and the presence of 400 mM NaCl or 20% 1,6-HD. Scale bar denotes 20 µm (A, C and D)

Factors stabilizing the coacervate formed by FcB(L17E)$_3$ to establish cytosolic Alexa488-IgG delivery

The following studies identified factors important for coacervate formation to elucidate the critical role of Alexa Fluor 488 labeling of IgG. In marked contrast to the mixture of FcB(L17E)$_3$ with Alexa488-IgG (CLSM analysis in Fig. 4A, right), no LLPS formation was observed when non-labeled IgG was used (Fig. 4A, left). This was also supported by the absorbance at 650 nm of the mixture of FcB(L17E)$_3$ with non-labeled

IgG (Fig. 4B, left), in which a marginal level of absorbance was evident compared with the mixture of FcB(L17E)$_3$ and Alexa488-IgG (Fig. 4B, right). Lysine residues of IgG were labeled with Alexa Fluor 488 5-sulfodichlorophenol (SDP) ester. This resulted in IgG with negatively charged and aromatic residues. FcB(L17E)$_3$ contains positively charged 15 lysine and one arginine residue together with 15 aromatic residues. Therefore, the possible interaction of FcB(L17E)$_3$ and Alexa488-IgG, including electrostatic interaction, π-π stacking, and cation-π stacking, may allow LLPS.

Unexpectedly, the FcB segment or binding of (L17E)$_3$ to IgG were not indispensable for liquid droplet formation and intracellular Alexa488-IgG delivery. Using (L17E)$_3$, which lacks the HWRGWV sequence of FcB(L17E)$_3$ (Table S1), droplets were formed in 25 mM HEPES (pH 7.5) when mixed with Alexa488-IgG (Fig. 4D; (L17E)$_3$), although the stability in NaCl was much lower than that of FcBP, yielding marginal absorption at 650 nm (Fig. 4C; (L17E)$_3$). Delivery of Alexa488-IgG to the cytosol was evident in approximately 10% of cells, which was considerably lower than the efficacy resulting from the use of FcBP (Fig. 4E and F; (L17E)$_3$).

Considering the contribution of electrostatic, π-π, and cation-π interactions to droplet formation, we prepared (L17E)$_3$ tagged with KRGFYY [KRGFYY(L17E)$_3$] (Table S1). KRGFYY-NH_2 is a control peptide used in the original study. The peptide has

no binding affinity to the Fc region, but contains aromatic and basic amino acids, similar to the FcBP segment.[7] KRGFYY(L17E)$_3$ also formed coacervates with Alexa488-IgG with less tolerance to NaCl (Fig. 4C and D; KRGFYY(L17E)$_3$), with approximately 2/3 absorption at 150 mM NaCl compared with that produced by the use of FcBP(L17E)$_3$. Notably, the efficacy of cytosolic Alexa488-IgG distribution was comparable to that of droplets formed from KRGFYY(L17E)$_3$ and Alexa488-IgG (Fig. 4E and F; KRGFYY(L17E)$_3$).

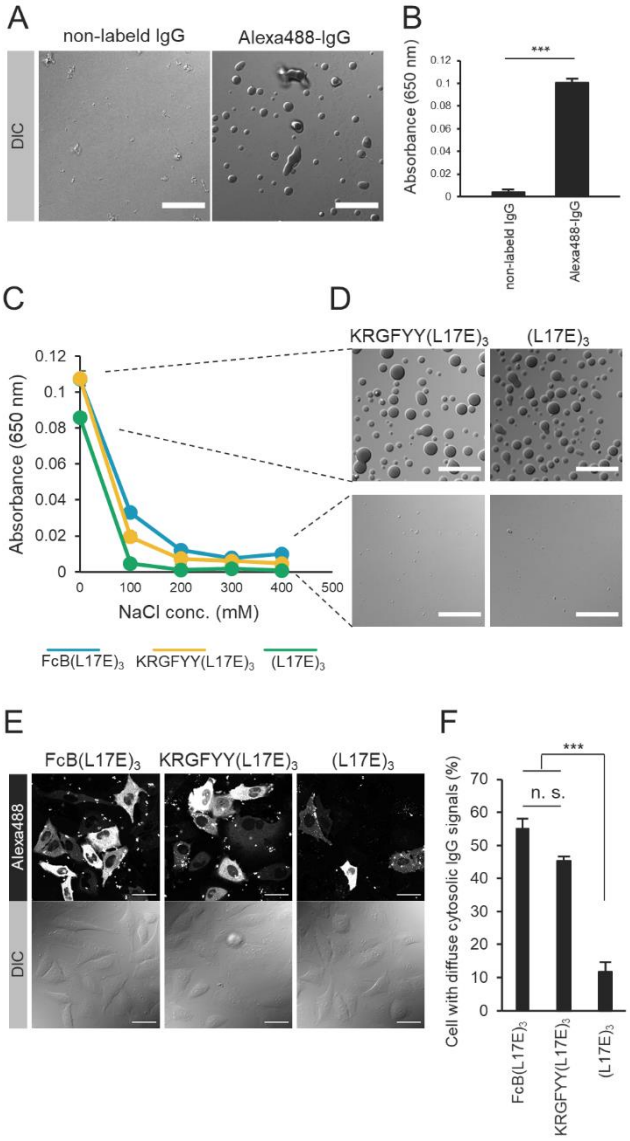

Figure 4. A, B) Importance of labeling of IgG with Alexa Fluorophore for liquid droplet formation with FcB(L17E)$_3$ and the intracellular delivery. A) DIC image and B) the absorbance at 650 nm of the solution of a mixture of non-labeled IgG (left) and Alexa488-IgG (right) with FcB(L17E)$_3$ in 25 mM HEPES buffer (pH 7.5). Results are presented as mean ± standard division (SD) (n=3). ***; $p<0.001$ by Student‘s t-test. C) The absorbance at 650 nm of the solution of the mixture of Alexa488-IgG with FcB(L17E)$_3$,

KRGFYY(L17E)$_3$, or (L17E)$_3$ in the absence and presence of NaCl. D) DIC images of the droplets in the absence and the presence of 400 mM of NaCl. E) The cytosolic appearance of Alexa488-IgG after treatment with the mixtures with 1 μM of FcB(L17E)$_3$, KRGFYY(L17E)$_3$, and (L17E)$_3$ for 30 min. F) Percentages of cells bearing diffuse cytosolic Alexa488-IgG signals. Results are presented as mean ± SE (n=3). ***; $p<0.001$, n.s.; not significantly different by Tukey-Kramer's honestly significant difference test. Scale bar denotes 20 μm (A, D) and 40 μm (E).

Possible delivery of other negatively charged proteins by FcB(L17E)$_3$

The absence of an Fc binding peptide in FcB(L17E)$_3$ to form liquid droplets with Alexa488-IgG suggested the possible applicability of liquid droplet-mediated intracellular delivery to other proteins. We hypothesized that electrostatic interactions between negatively charged Alexa488 moieties and positively charged FcB(L17E)$_3$ would contribute to liquid droplet formation. Accordingly, we examined droplet formation and intracellular delivery using a supernegatively charged green fluorescent protein ((−30)GFP). This version of GFP is an engineered GFP with an unusually high net negative theoretical charge of –30.[22] The nuclear localization signal (NLS) derived from the SV40 large T antigen (PKKKRKV)[23] was added to the (−30)GFP to generate

NLS-(−30)GFP.[24] Cytosolic translocation of NLS-(−30)GFP should lead to nuclear accumulation of the protein, and thus internalization could be analyzed in terms of fluorescence signals localized in the nucleus. As a control, enhanced GFP (EGFP)[25] with a net charge of +2 (nearly neutral) was employed, and NLS-tagged protein (NLS-EGFP) were similarly prepared.

Liquid droplet formation of these proteins in the presence of FcB(L17E)$_3$ was then evaluated by CLSM imaging. Although the droplet size was smaller compared with the use of Alexa488-IgG, robust formation of liquid droplets was observed by CLSM analysis of the mixture of NLS-(−30)GFP with FcB(L17E)$_3$ (Fig. 5A, right). In contrast, few liquid droplets were observed in the case of NLS-EGFP (Fig. 5A, left). The absorbance of these mixtures at 650 nm was consistent with the CLSM observations (Fig. 5B). Collapse at elevated NaCl concentrations is a criterion for LLPS. This was confirmed for the droplets formed by the mixture of FcB(L17E)$_3$ and NLS-(−30)GFP (Fig. 5C). This result suggests that electrostatic interactions between the negative charges of a protein of interest and positively charged FcB(L17E)$_3$ are important for the formation of liquid droplets.

Liquid droplets formed with FcB(L17E)$_3$ facilitated the delivery of NLS-(−30)GFP into the cytosol. Nuclear localization of NLS-(−30)GFP signals were observed

for >50% of the cells treated with a mixture of 75 μg/mL NLS-(−30)GFP with 1 μM of FcB(L17E)$_3$ (i.e., the same weight of protein over FcB(L17E)$_3$ as used for liquid droplet formation using Alexa488-IgG; Fig. 5D and E, right). However, the mixture with NLS-EGFP, which did not lead to liquid droplet formation, yielded poor internalization (Fig. 5D and E, left).

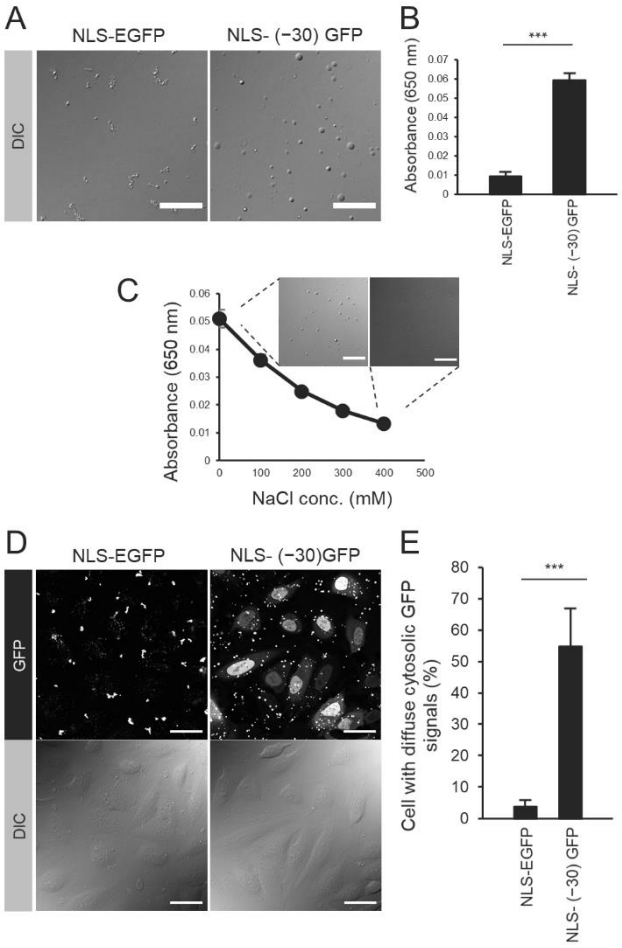

Figure 5. A) DIC images and B) absorbance at 650 nm of the mixture of NLS-EGFP (left) and NLS-(−30)GFP (right) with FcB(L17E)$_3$ in 25 mM HEPES buffer (pH 7.5). C)

Absorbance at 650 nm of the solution containing FcB(L17E)$_3$ and (−30)GFP with various concentrations of NaCl. (Inset) DIC images of the solution in the absence and presence of 400 mM NaCl. D) The cytosolic appearance of NLS-EGFP and NLS-(-30)GFP after treatment with 1 μM of FcB(L17E)$_3$ for 30 min. E) Percentages of cells bearing diffuse cytosolic NLS-EGFP (left) or NLS-(−30)GFP (right) signals. Results are presented as mean ± standard deviation (SD) (B) or SE (E) (n=3). ***; $p<0.001$ by Student's t-test (B, E). Scale bar denotes 20 μm (A, C) and 40 μm (D).

The above results suggest the possibility of delivering negatively charged proteins into the cytosol through liquid droplets formed with FcB(L17E)$_3$. To further confirm the validity of this assumption, we examined whether monoclonal anti-nuclear pore complex (NPC)-IgG modified with Alexa Fluor 594 (Alexa594-anti-NPC-IgG) could be delivered into the cytosol to target NPC using FcB(L17E)$_3$. NPC, which is located on the nuclear membrane, is a large protein complex in cells. It plays a key role in exchanging components between the cytoplasm and nucleus.[26] Alexa Fluor 594 bears two negative charges as in the case of Alexa Fluor 488, and modification with IgG may promote liquid droplet formation. Control IgG labeled with Alexa Fluor 594, which lacks NPC targeting ability, was also prepared (Alexa594-IgG).

HeLa cells were similarly treated with a mixture of Alexa594-anti-NPC-IgG or Alexa594-IgG with FcB(L17E)$_3$ for 30 min, using the mixtures with Alexa488-IgG, followed by Hoechst33342 staining of the nucleus without fixation of the cells and CLSM observation (Fig. 6A). Successful cytosolic delivery of IgGs was achieved using both mixtures. However, a significant accumulation on the nuclear membrane was only observed when Alexa594-anti-NPC-IgG was used, indicating that IgG delivered into the cytosol by FcB(L17E)$_3$ maintained its functionality to target subcellular components in living cells.

We also explored the possibility of delivering functional proteins without chemical modification with fluorescent molecules, but using a negatively charged protein tag. The tag was (−30)GFP, which was efficiently internalized into cells by complex formation with FcB(L17E)$_3$. An anti-mCherry nanobody[27] was employed as a model functional protein to be delivered into the cytosol. Nanobodies are derived from the VHH segment of heavy-chain antibodies of Camelidae. They have a much smaller molecular size than IgG.[28] Thus, nanobodies are considered a promising molecular form in antibody therapies.

Anti-mCherry-nanobody fused with (−30)GFP (anti-mChNB-(−30)GFP) successfully targeted intracellularly expressed mCherry. HeLa cells stably expressing

lifeact-mCherry were incubated with a mixture of anti-mChNB-(−30)GFP and FcB(L17E)$_3$ for 30 min. Significant colocalization of anti-mChNB-(−30)GFP signals with Lifeact-mCherry suggested the cytosolic translocation of anti-mChNB-(−30)GFP and successful targeting of the cellular protein of interest. (Fig. 6B). The (−30)GFP not fused to anti-mChNB was also delivered into cells. The result was a diffuse cytosolic distribution with no significant colocalization with the actin cytoskeleton, indicating the retention of target recognition ability in anti-mChNB delivered into cells.

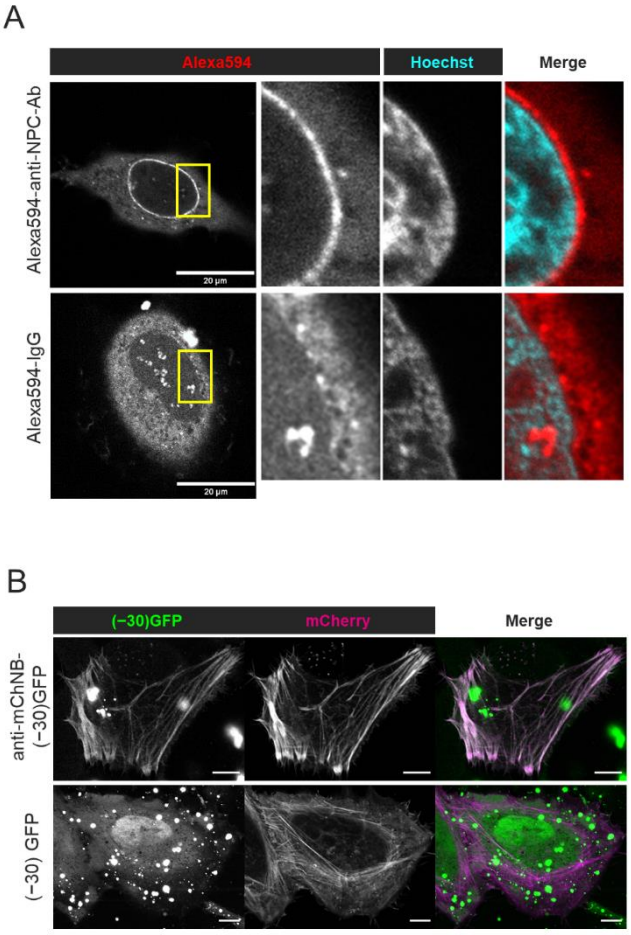

Figure 6. A) Localization of Alexa594-anti-NPC IgG, but not Alexa594-IgG, on nuclear membranes following incubation with $FcB(L17E)_3$. B) Cellular localization of anti-mCherry-nanobody-(−30)GFP and (−30)GFP in Lifeact-mCherry expressing cells following incubation with $FcB(L17E)_3$. Scale bar denotes 20 µm.

Conclusion

A mixture of Alexa488-IgG and FcB(L17E)$_3$ formed liquid droplets. Rapid influx of Alexa488-IgG was attained by the cellular attachment of liquid droplets. Alexa488-IgG distribution throughout the cells resulted in approximately 1 min. Notably, this influx was attained in a medium containing 10% serum. Negative charges cast on IgG by modification with Alexa Fluor 488 play a role in droplet formation. More interestingly, in the binding of FcB(L17E)$_3$ to IgG, the FcBP segment was not necessarily needed, but it seems likely that some hydrophobicity and basicity of the segment are important for liquid droplet formation. In particular, electrostatic interactions are likely crucial for liquid droplet formation using FcB(L17E)$_3$. Based on the above findings, other proteins modified with negatively charged moieties or fused with a negatively charged protein tag were also delivered into the cell interior with the help of FcB(L17E)$_3$. Importantly, the IgG and nanobody delivered into cells retained their ability to bind their target proteins in the cells. This suggests the potential applicability of the FcB(L17E)$_3$ mediated approach for intracellular delivery of a wide variety of proteins or other macromolecules with appropriate modifications.

Studies on the mode of action of the FcB(L17E)$_3$-mediated cytosolic IgG delivery, accompanied by uptake inhibition by the treatment of CytoD, EIPA, and

wortmannin, suggested the possible involvement of membrane ruffling driven by actin polymerization and induction of macropinocytosis-like uptake machinery (Fig. 7). Further studies are needed to elucidate the exact modes and stages of membrane translocation to attain cytosolic IgG translocation. However, considering that the cytosolic IgG translocation was completely abolished at 4°C (i.e., the temperature at which ATP-driven cellular machineries do not operate), translocation should not be achieved by simple pore formation in cell membranes. There is a significant contribution of cellular energy-dependent mechanisms induced by the interaction of liquid droplets containing FcB(L17E)$_3$ with cells.

The concept of coacervation or LLPS was established in the early 1930s.[16] However, in recent years, the importance of LLPS by proteins and RNAs in various cellular functions and regulation has become established as a new research field in life science. Although LLPS is also considered to have considerable potential in the intracellular delivery of biomacromolecules, including in formulation, only a limited number of reports of its successful application in protein delivery have been published. To our knowledge, this study shows for the first time that large biomacromolecules, such as antibodies, can be delivered into the cytosol through coacervation using a peptide. Further consideration of the design of liquid droplet composition and elucidation of the

mechanisms allowing cytosolic delivery will open new doors for material transfer into cells.

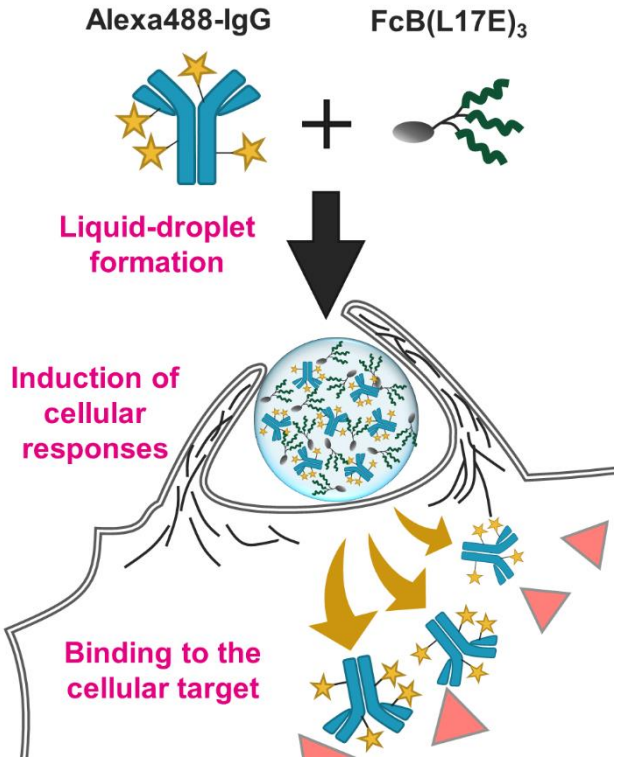

Figure 7. Proposed mechanism of action of FcB(L17E)$_3$. FcB(L17E)$_3$ interacts with negatively charged proteins by electrostatic interaction followed by induction of LLPS and formation of coacervates. LLPS condenses proteins into coacervates. Coacervates containing L17E domain are able to access the cell membrane. The attachment of liquid droplets to the cell membrane induces actin-reorganization and membrane ruffling, possibly leading to transient membrane permeabilization. Successful cytosolic delivery of Alexa-IgG leads to interaction with the cellular targets.

Acknowledgement

This work was supported by JSPS KAKENHI (Grant Numbers JP18H04017, JP20H04707, JP21H04794), and by JST CREST (Grant Number JPMJCR18H5). K.S., Y. H., and M. A. are grateful for the JSPS Research Fellowship for Young Scientists.

References

[1] a) K. Singh, W. Ejaz, K. Dutta, S. Thayumanavan, *Bioconjug. Chem.* **2019**, *30*, 1028-1041; b) P. D. Kaiser, J. Maier, B. Traenkle, F. Emele, U. Rothbauer, *Biochim. Biophys. Acta* **2014**, *1844*, 1933-1942; c) S. Guillard, R. R. Minter, R. H. Jackson, *Trends Biotechnol.* **2015**, *33*, 163-171.

[2] a) D. Schumacher, J. Helma, A. F. L. Schneider, H. Leonhardt, C. P. R. Hackenberger, *Angew. Chem. Int. Ed. Engl.* **2018**, *57*, 2314-2333; b) T. Romer, H. Leonhardt, U. Rothbauer, *Curr. Opin. Biotechnol* .**2011**, *22*, 882-887; c) A. Beck, L. Goetsch, C. Dumontet, N. Corvaïa, *Nat. Rev. Drug Discov.* **2017**, *16*, 315-337.

[3] a) A. Erazo-Oliveras, K. Najjar, L. Dayani, T. Y. Wang, G. A. Johnson, J. P. Pellois, *Nat. Methods* **2014**, *11*, 861-867; b) E. I. Ozay, G. Gonzalez-Perez, J. A. Torres, J. Vijayaraghavan, R. Lawlor, H. L. Sherman, D. T. Garrigan, Jr., A. S. Burnside, B. A. Osborne, G. N. Tew, L. M. Minter, *Mol. Ther.* **2016**, *24*, 2118-2130; c) A. Abraham, U. Natraj, A. A. Karande, A. Gulati, M. R. Murthy, S. Murugesan, P. Mukunda, H. S. Savithri, *Sci. Rep.* **2016**, *6*, 21803; d) Y. Kondo, K. Fushikida, T. Fujieda, K. Sakai, K. Miyata, F. Kato, M. Kato, *J. Immunol. Methods* **2008**, *332*, 10-17; e) S. Niamsuphap, C. Fercher, S. Kumble, P. Huda, S. M. Mahler, C. B. Howard, *Expert Opin. Drug Deliv.* **2020**, *17*, 1189-1211; f) S. Du, S. S. Liew, C. W. Zhang, W. Du, W. Lang, C. C. Y. Yao, L. Li, J. Ge, S. Q. Yao, *ACS Cent. Sci.* **2020**, *6*, 2362-2376; g) Y. Lee, T. Ishii, H. J. Kim, N. Nishiyama, Y. Hayakawa, K. Itaka, K. Kataoka, *Angew. Chem. Int. Ed. Engl.* **2010**, *49*, 2552-2555; h) S. M. Shin, D. K. Choi, K. Jung, J. Bae, J. S. Kim, S. W. Park, K. H. Song, Y. S. Kim, *Nat. Commun.* **2017**, *8*, 15090; i) H. D. Herce, D. Schumacher, A. F. L. Schneider, A. K. Ludwig, F. A. Mann, M. Fillies, M. A. Kasper, S. Reinke, E. Krause, H. Leonhardt, M. C. Cardoso, C. P. R. Hackenberger, *Nat. Chem.* **2017**, *9*, 762-771; j) S. Itakura, S. Hama, H. Ikeda, N. Mitsuhashi, E. Majima, K. Kogure, *FEBS J.* **2015**, *282*, 142-152; k) H. H. Wang, A. Tsourkas, *Proc. Natl. Acad Sci. U. S. A.* **2019**, *116*, 22132-22139; l) J. V. V. Arafiles, H. Hirose, M. Akishiba, S. Tsuji, M. Imanishi, S. Futaki, *Bioconjug. Chem.* **2020**, *31*, 547-553; m) K. A. Mix, J. E. Lomax, R. T. Raines, *J. Am. Chem. Soc.* **2017**, *139*, 14396-14398; n) Y. W. Lee, D. C. Luther, R. Goswami, T. Jeon, V. Clark, J. Elia, S. Gopalakrishnan, V. M. Rotello, *J. Am. Chem. Soc.* **2020**, *142*, 4349-4355; o) S. Y. Kim, A. N. Bondar, W. C. Wimley, K. Hristova, *Biophys. J.* **2021**, *120*, 618-630, and references cited therein.

[4] a) M. Akishiba, T. Takeuchi, Y. Kawaguchi, K. Sakamoto, H. H. Yu, I. Nakase, T. Takatani-Nakase, F. Madani, A. Gräslund, S. Futaki, *Nat. Chem.* **2017**, *9*, 751-761; b) M. Akishiba, S. Futaki, *Mol. Pharm.* **2019**, *16*, 2540-2548; c) N. Tamemoto, M. Akishiba, K.

Sakamoto, K. Kawano, H. Noguchi, S. Futaki, *Mol. Pharm.* **2020**; d) K. Sakamoto, M. Akishiba, T. Iwata, K. Murata, S. Mizuno, K. Kawano, M. Imanishi, F. Sugiyama, S. Futaki, *Angew. Chem. Int. Ed. Engl.* **2020**; e) Y. Nomura, K. Sakamoto, M. Akishiba, T. Iwata, H. Hirose, S. Futaki, *Bioorg. Med. Chem. Lett.* **2020**, *30*, 127362; f) H.-H. Yu, K. Sakamoto, M. Akishiba, N. Tamemoto, H. Hirose, I. Nakase, M. Imanishi, F. Madani, A. Gräslund, S. Futaki, *Peptide Science* **2020**, *112*, e24144; g) K. Sakamoto, M. Akishiba, T. Iwata, J. V. V. Arafiles, M. Imanishi, S. Futaki, *Bioorg. Med. Chem. Lett.* **2021**, *40*, 127925; h) S. Futaki, J. V. V. Arafiles, H. Hirose, *Chemistry Letters* **2020**, *49*, 1088-1094.

[5] L. Yan, M. E. Adams, *J. Biol. Chem.* **1998**, *273*, 2059-2066.

[6] a) E. N. Lorenzon, J. P. Piccoli, N. A. Santos-Filho, E. M. Cilli, *Protein Pept. Lett.* **2019**, *26*, 98-107; b) W. Y. Hsu, T. Masuda, S. Afonin, T. Sakai, J. V. V. Arafiles, K. Kawano, H. Hirose, M. Imanishi, A. S. Ulrich, S. Futaki, *Bioorg Med Chem Lett* **2020**, *30*, 127190; c) C. Díaz-Perlas, B. Oller-Salvia, M. Sánchez-Navarro, M. Teixidó, E. Giralt, *Chem. Sci.* **2018**, *9*, 8409-8415; d) D. J. Brock, L. Kustigian, M. Jiang, K. Graham, T. Y. Wang, A. Erazo-Oliveras, K. Najjar, J. Zhang, H. Rye, J. P. Pellois, *Traffic* **2018**, *19*, 421-435.

[7] H. Yang, P. V. Gurgel, R. G. Carbonell, *J. Pept. Res.* **2005**, *66*, 120-137.

[8] K. Yamada, Y. Ito, *ChemBioChem* **2019**, *20*, 2729-2737.

[9] S. Futaki, K. Kitagawa, *Tetrahedron Lett.* **1994**, *35*, 1267-1270.

[10] M. Ishiyama, Y. Miyazono, K. Sasamoto, Y. Ohkura, K. Ueno, *Talanta* **1997**, *44*, 1299-1305.

[11] J. Riedl, A. H. Crevenna, K. Kessenbrock, J. H. Yu, D. Neukirchen, M. Bista, F. Bradke, D. Jenne, T. A. Holak, Z. Werb, M. Sixt, R. Wedlich-Soldner, *Nat. Methods* **2008**, *5*, 605-607.

[12] A. J. Ridley, *BioEssays* **1994**, *16*, 321-327.

[13] L. A. Selden, L. C. Gershman, J. E. Estes, *Biochem. Biophys. Res. Commun.* **1980**, *95*, 1854-1860.

[14] O. Meier, K. Boucke, S. V. Hammer, S. Keller, R. P. Stidwill, S. Hemmi, U. F. Greber, *J. Cell Biol.* **2002**, *158*, 1119-1131.

[15] N. Araki, M. T. Johnson, J. A. Swanson, *J. Cell Biol.* **1996**, *135*, 1249-1260.

[16] a) N. R. Johnson, Y. Wang, *Expert Opin. Drug Deliv.* **2014**, *11*, 1829-1832; b) L. Zhou, H. Shi, Z. Li, C. He, *Macromol. Rapid Commun.* **2020**, *41*, e2000149; c) S. Muniyandy, T. Sathasivam, A. K. Veeramachineni, P. Janarthanan, *Polymers* **2015**, *7*, 1088-1105; d) G. O. S. Huei, S. Muniyandy, T. Sathasivam, A. K. Veeramachineni, P. Janarthanan, *Chemical Papers* **2016**, *70*, 243-252.

[17] S. Boeynaems, S. Alberti, N. L. Fawzi, T. Mittag, M. Polymenidou, F. Rousseau, J. Schymkowitz, J. Shorter, B. Wolozin, L. Van Den Bosch, P. Tompa, M. Fuxreiter, *Trends*

Cell Biol. **2018**, *28*, 420-435.

[18] Y. Shin, J. Berry, N. Pannucci, M. P. Haataja, J. E. Toettcher, C. P. Brangwynne, *Cell* **2017**, *168*, 159-171.e114.

[19] a) T. P. Dao, R. M. Kolaitis, H. J. Kim, K. O'Donovan, B. Martyniak, E. Colicino, H. Hehnly, J. P. Taylor, C. A. Castañeda, *Mol. Cell* **2018**, *69*, 965-978.e966; b) T. J. Nott, E. Petsalaki, P. Farber, D. Jervis, E. Fussner, A. Plochowietz, T. D. Craggs, D. P. Bazett-Jones, T. Pawson, J. D. Forman-Kay, A. J. Baldwin, *Mol. Cell* **2015**, *57*, 936-947; c) Y. Lin, E. Mori, M. Kato, S. Xiang, L. Wu, I. Kwon, S. L. McKnight, *Cell* **2016**, *167*, 789-802.E12.

[20] D. Priftis, M. Tirrell, *Soft Matter* **2012**, *8*, 9396-9405.

[21] N. O. Taylor, M. T. Wei, H. A. Stone, C. P. Brangwynne, *Biophys. J.* **2019**, *117*, 1285-1300.

[22] M. S. Lawrence, K. J. Phillips, D. R. Liu, *J. Am. Chem. Soc.* **2007**, *129*, 10110-10112.

[23] D. Kalderon, B. L. Roberts, W. D. Richardson, A. E. Smith, *Cell* **1984**, *39*, 499-509.

[24] J. V. V. Arafiles, H. Hirose, Y. Hirai, M. Kuriyama, M. M. Sakyiamah, W. Nomura, K. Sonomura, M. Imanishi, A. Otaka, H. Tamamura, S. Futaki, *Angew. Chem. Int. Ed. Engl. 60*, 11928-11936.

[25] T. T. Yang, L. Cheng, S. R. Kain, *Nucleic Acids Res.* **1996**, *24*, 4592-4593.

[26] C. Strambio-De-Castillia, M. Niepel, M. P. Rout, *Nat. Rev. Mol. Cell Biol.* **2010**, *11*, 490-501.

[27] Y. Katoh, M. Terada, Y. Nishijima, R. Takei, S. Nozaki, H. Hamada, K. Nakayama, *J. Biol. Chem.* **2016**, *291*, 10962-10975.

[28] E. Beghein, J. Gettemans, *Front. Immunol.* **2017**, *8*, 771.

Table of contents

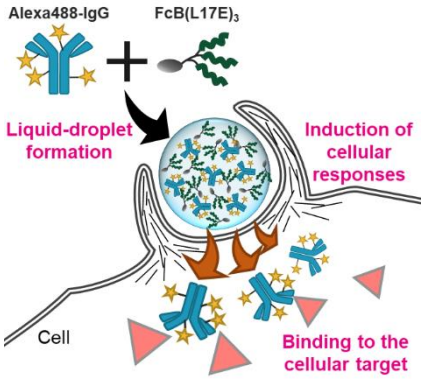

Fc region binding peptide conjugated with attenuated lytic peptide L17E trimer [FcB(L17E)$_3$] was designed for intracellular delivery of IgG. Liquid droplets were formed by mixing Alexa Fluor 488 labeled IgG (Alexa488-IgG) with FcB(L17E)$_3$. Droplet contact with cell membrane led to quick influx of Alexa488-IgG throughout cells. Successful delivery of functional proteins into cells allowed binding to subcellular targets in the presence of FcB(L17E)$_3$.